Performance Improvement of Power System Stability by Using Multiple Damping Controllers Based on PSS and the UPFC

A. N. Hussain[#1], F. Malek[#2], M. A. Rashid[#3], M. F. Haji Abd Malek[*4]
[#] School of Electrical Systems Engineering, University Malaysia Perlis (UniMAP)
Pauh, Arau, Perlis,Malaysia
[1] alinasser1974@yahoo.com
[2] mfareq@unimap.edu.my.edu
[3] rashid68@yahoo.com
[*] MISC LNG Liaison Office Japan
Yokonama, Japan
[4] farizmalek@gmail.com

Abstract—**Enhancement of stability of the power system has been achieved by the application of Unified power flow controller (UPFC) device with an additional supplementary controller. This supplementary damping controller can be installed on any control channel of the UPFC inputs to implement the task of power oscillation damping (POD) controller. We have presented a comprehensive assessment and performed analytical study through simulation of the damping function of the multiple damping controllers. Dual and triple-coordinated design among power system stabilizer (PSS) and different UPFC-POD controllers were considered in order to identify the design that provided the most robust damping performance in a single machine infinite bus (SMIB). The parameters of the damping controller were tuned in the individual and coordinated design by using a chaotic particle swarm optimization (CPSO) algorithm that optimized the given eigenvalue-based objective function. The simulation results demonstrate that the proposed dual and triple-coordinated designs provide higher damping of Low-frequency oscillations and improve the system damping over their individual control responses.**

Keyword-Power system stability, Transmission lines, Flexible ac transmission systems, Power system stabilizer, Coordinated design

I. INTRODUCTION

Electric power system becomes more heavily loaded over long distances because of economic and environmental pressures as a result, undesirable electromechanical oscillations happen more often than before [1], [2]. In absence of sufficient damping these oscillations may develop. The oscillations can cause system separation in the low frequency range of 0.1–2 Hz [3], [4].

In past decades, PSSs were appeared as an economic and effective technique to add damping to the power system oscillations for the nominal system parameters and nominal operating condition. However, the performance of the system deteriorated while the system operating conditions were varied in a large scale [5]-[7]. Therefore, with these limitations the use of PSS alone cannot provide adequate damping for the low-frequency oscillation problems [8].

Flexible ac transmission system (FACTS) devices provide the controllability and flexibility for power system operations to achieve the full utilization of the existing power systems [9], [10]. Recently UPFC device has attracted more attention of the researchers than any other devices of the FACTS family because it can provide a full compensation. These compensations were provided in terms of voltage and phase shifting regulation, impedance and reactive compensation [11], [12]. Besides these primary control functions, it also is capable of enhancing the power system stability by the addition of a supplementary damping controller, which can be installed on any control channel of the UPFC inputs to implement the task of power oscillation damping (POD) controller [13].

To improve overall system performance, the technique that is most often used is to arrange multiple damping controllers, but the interaction among them may cause destabilization of the damping of the oscillations of the system. In order to overcome the problem of interactions among multiple damping controllers, a coordinated design is required to gain the benefits of multiple stabilizers, thereby enhancing the stability of the system and to

reduce any possible negative interactions among the different stabilizers. Many researches have proposed the coordination between PSSs and FACTS devices with POD controllers [14]-[16].

Parameter tuning is the key problem in the coordinated design, because the effectiveness of coordinated design in damping of oscillations is based on optimal parameters of the multiple damping controllers. Hence, the use of optimization techniques must be efficient and quick, and it must ensure the security of dynamic system in case of critical events. Many artificial intelligence techniques have been used to provide the desired coordinated design and robustness of multiple stabilizers, including the application of artificial neural networks [17], [18], genetic algorithms [8], [19], fuzzy logic control [20], [21], bacterial foraging algorithm [22], and various combinations of these approaches [23], [24].

In the last few decades, the particle swarm optimization (PSO) technique has appeared as a useful tool to produce excellent solutions in short time for solving optimization problem. Many researchers have been adopted PSO technique [25]-[27]. The simple PSO depends on the tuning parameters significantly. But it is not assured that it will be a global convergent. To improve the global searching ability and prevent a slide into the premature convergence to local minima, a chaotic particle swarm optimization (CPSO) technique by combining the PSO with chaotic sequence techniques.

In this paper, we have presented the results of our comprehensive comparison and assessment of the damping function of multiple damping stabilizers using different coordinated designs in order to identify the design that provided the most effective damping performance. The two alternative designs we evaluated are listed below:

- Dual-coordinated design between PSS and any one out from the four inputs controls channels of the series and shunt structure of UPFC device, because any control loop can superimpose a supplementary damping controller to implement the required damping.
- Triple-coordinated design among PSS and any two different out from the four inputs controls channels of the UPFC device.

The CPSO technique was used for tuning the parameters of the multiple damping stabilizers in the coordinated design based on an eigenvalue objective function. Simulation results for a SMIB equipped with UPFC device shows that, the dual and triple-coordinated design has better damping ability for low frequency oscillations (LFO) than their individual control responses, which improves the stability of the power system significantly.

II. MATHEMATICAL MODEL FOR SMIB EQUIPPED WITH UPFC OF POWER SYSTEM

Fig. 1 shows the application of UPFC device in SMIB power system to increase the controllability and flexibility. The UPFC is composed of two three-phase GTO based voltage source converters. One of the voltage source converters (VSC-1) is connected in shunt and the other one (VSC-2) is connected in series. These two voltage source converters are coupled by a common dc link and each converter is connected to the transmission line through an excitation transformer (ET) and a boosting transformer (BT) in order to maintain bi-directional power flow between the series and shunt converters. The four input control signals to the UPFC are the amplitude of modulation ratio and phase angle signals of each converter. These are denoted as m_E, m_B, δ_E and δ_B respectively. These parameters are considered as UPFC control inputs to provide synchronized power compensation in series line without external voltage source [5], [28].

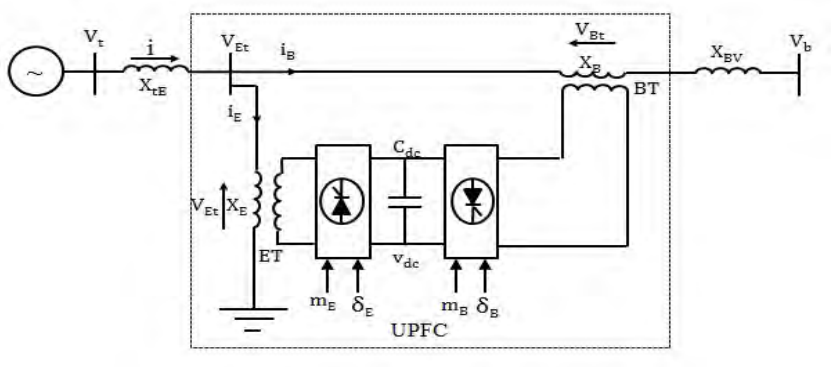

Fig. 1. SMIB power system equipped with UPFC.

A. Nonlinear Dynamic Model of UPFC

The dynamic model of the UPFC is required to investigate the effect of the UPFC to enhance the small signal stability of the power system. By applying Park's transformation and neglecting the resistance and transients of the ET and BT transformers, the UPFC can be modeled as [1]:

$$\begin{bmatrix} v_{Etd} \\ v_{Etq} \end{bmatrix} = \begin{bmatrix} 0 & -x_E \\ x_E & 0 \end{bmatrix} \begin{bmatrix} i_{Ed} \\ i_{Eq} \end{bmatrix} + \begin{bmatrix} m_E v_{dc} \cos \delta_E/2 \\ m_E v_{dc} \sin \delta_E/2 \end{bmatrix} \quad (1)$$

$$\begin{bmatrix} v_{Btd} \\ v_{Btq} \end{bmatrix} = \begin{bmatrix} 0 & -x_B \\ x_B & 0 \end{bmatrix} \begin{bmatrix} i_{Bd} \\ i_{Bq} \end{bmatrix} + \begin{bmatrix} m_B v_{dc} \cos \delta_B/2 \\ m_B v_{dc} \sin \delta_B/2 \end{bmatrix} \quad (2)$$

$$\dot{v}_{dc} = (3m_E/4C_{dc})[\cos \delta_E \quad \sin \delta_E] \begin{bmatrix} i_{Ed} \\ i_{Eq} \end{bmatrix} + (3m_B/4C_{dc})[\cos \delta_B \quad \sin \delta_B] \begin{bmatrix} i_{Bd} \\ i_{Bq} \end{bmatrix} \quad (3)$$

where v_{Et}, i_E and x_E are the excitation transformer voltage, current and reactance, respectively; v_{Bt}, i_B and x_B are the boosting transformer voltage, current and reactance, respectively; v_{dc} and C_{dc} are the DC-link voltage and capacitance, respectively.

From Fig. 1, we can have:

$$\bar{v}_t = jx_{tE}\bar{\imath} + \bar{v}_{Et} \quad (4)$$

$$\bar{v}_{Et} = \bar{v}_{Bt} + jx_{Bv}\bar{\imath}_B + \bar{v}_b \quad (5)$$

$$\bar{\imath} = \bar{\imath}_E + \bar{\imath}_B \quad (6)$$

where i, v_t and v_b are the armature current, generator terminal voltage and infinite bus voltage, respectively; x_{tE} and x_{Bv} are transmission line reactance's, respectively. Equations (4) and (5) can be expressed in the d-q axis reference frame as

$$v_{td} + jv_{tq} = jx_{tE}\big(i_{Ed} + ji_{Eq} + i_{Bd} + ji_{Bq}\big) + v_{Etd} + jv_{Etq} = x_q\big(i_{Eq} + i_{Bq}\big) + j\big[\grave{E}_q - \grave{x}_d(i_{Ed} + i_{Bd})\big] \quad (7)$$

$$v_{Etd} + jv_{Etq} = v_{Btd} + jv_{Btq} + jx_{Bv}i_{Bd} - x_{Bv}i_{Bq} + v_b \sin \delta + jv_b \cos \delta \quad (8)$$

From equations (1), (2), (7), and (8) can be obtained the equation's current injection:

$$i_{Ed} = (x_{BZ}/x_{dZ})\grave{E}_q - (x_{Bd}/x_{dZ})(v_{dc}m_E \sin \delta_E/2) + (x_{dE}/x_{dZ})[v_b \cos \delta + (v_{dc}m_B \sin \delta_B/2)] \quad (9)$$

$$i_{Eq} = \big(x_{Bq}/x_{qZ}\big)(v_{dc}m_E \cos \delta_E/2) - \big(x_{qE}/x_{qZ}\big)[v_b \sin \delta + (v_{dc}m_B \cos \delta_B/2)] \quad (10)$$

$$i_{Bd} = (x_E/x_{dZ})\grave{E}_q - (x_{dE}/x_{dZ})(v_{dc}m_E \sin \delta_E/2) - (x_{dt}/x_{dZ})[v_b \cos \delta + (v_{dc}m_B \sin \delta_B/2)] \quad (11)$$

$$i_{Bq} = \big(x_{qE}/x_{qZ}\big)(-v_{dc}m_E \cos \delta_E/2) + \big(x_{qt}/x_{qZ}\big)[(v_b \sin \delta) + (v_{dc}\, m_B \cos \delta_B/2)] \quad (12)$$

where:

$$x_{BZ} = x_B + x_{Bv}, \quad x_{dZ} = (\grave{x}_d + x_{tE} + x_E)(x_B + x_{Bv}) + x_E(\grave{x}_d + x_{tE})$$

$$x_{Bd} = x_B + x_{Bv} + \grave{x}_d + x_{tE}, \quad x_{dE} = \grave{x}_d + x_{tE}, \quad x_{Bq} = x_B + x_{Bv} + x_q + x_{tE}$$

$$x_{qZ} = \big(x_q + x_{tE} + x_E\big)(x_B + x_{Bv}) + x_E\big(x_q + x_{tE}\big), \quad x_{dt} = (\grave{x}_d + x_{tE} + x_E)$$

$$x_{qE} = x_q + x_{tE}, x_{qt} = x_q + x_{tE} + x_E.$$

where x_d, $\grave{x}_d$ and x_q are the d-axis reactance, d-axis transient reactance and q-axis reactance, respectively.

B. Nonlinear Model of the Power System

The nonlinear model equations of the SMIB system as shown in Fig. 1 is described by [29]:

$$\dot{\delta} = \omega_b(\omega - 1) \quad (13)$$

$$\dot{\omega} = [P_m - P_e - D(\omega - 1)]/M \quad (14)$$

$$\dot{E}'_q = \left[E_{fd} - E_q\right]/\dot{T}_o \tag{15}$$

where ω_b is the synchronous speed; ω and δ are the rotor speed and angle, respectively; P_m and P_e are mechanical input and electrical output power of the generator, respectively; *M* and *D* are the machine inertia and damping coefficient, respectively; E_{fd}, E_q and $\dot{E}_q$ are the generator field voltage, generator internal voltage and transient generator internal voltage, respectively; $\dot{T}_o$ is the time constant of excitation circuit.

The excitation system is represented by a first order (IEEE type – ST1) [30].

$$\dot{E}_{fd} = \left[K_a\left(v_{ref} - v_t\right) - E_{fd}\right]/T_a \tag{16}$$

where v_{ref} is the reference voltage, $K_a$is the gain and T_a is the time constant of excitation system respectively.

The generator output power in terms of the d-axis and q-axis components of the terminal voltage vt and the armature current i is represented as follows:

$$P_e = v_{td}i_d + v_{tq}i_q \tag{17}$$

$$v_t = v_{td} + jv_{tq} \tag{18}$$

$$v_{td} = x_q i_q;\ v_{tq} = \dot{E}_q - \dot{x}_d i_d \tag{18a}$$

$$i = i_d + i_q \tag{19}$$

$$i_d = i_{Ed} + i_{Bd};\ i_q = i_{Eq} + i_{Bq} \tag{19a}$$

$$E_q = \dot{E}_q + i_d(x_d - \dot{x}_d) \tag{20}$$

C. Linearized Model of the Power System Equipped with UPFC

Linear dynamic model of the power system is obtained by linearizing the nonlinear equations (3-20) around nominal operating point. The linearized model of the power system as shown in Fig. 1 is given as follows:

$$\Delta\dot{\delta} = \omega_b\Delta\omega \tag{21}$$

$$\Delta\dot{\omega} = (-\Delta P_e - D\Delta\omega)/M \tag{22}$$

$$\Delta\dot{E}'_q = \left(-\Delta E_q + \Delta E_{fd}\right)/\dot{T}_{do} \tag{23}$$

$$\Delta\dot{E}_{fd} = \left(-K_a\Delta v_t - \Delta E_{fd}\right)/T_a \tag{24}$$

$$\Delta\dot{v}_{dc} = K_7\Delta\delta + K_8\Delta\dot{E}_q - K_9\Delta v_{dc} + K_{ce}\Delta m_E + K_{c\delta e}\Delta\delta_E + K_{cb}\Delta m_B + K_{c\delta b}\Delta\delta_B \tag{25}$$

$$\Delta P_e = K_1\Delta\delta + K_2\Delta\dot{E}_q + K_{pc}\Delta v_{dc} + K_{pe}\Delta m_E + K_{p\delta e}\Delta\delta_E + K_{pb}\Delta m_B + K_{p\delta b}\Delta\delta_B \tag{26}$$

$$\Delta\dot{E}_q = K_4\Delta\delta + K_3\Delta\dot{E}_q + K_{qc}\Delta v_{dc} + K_{qe}\Delta m_E + K_{q\delta e}\Delta\delta_E + K_{qb}\Delta m_B + K_{q\delta b}\Delta\delta_B \tag{27}$$

$$\Delta v_t = K_5\Delta\delta + K_6\Delta\dot{E}_q + K_{vc}\Delta v_{dc} + K_{ve}\Delta m_E + K_{v\delta e}\Delta\delta_E + K_{vb}\Delta m_B + K_{v\delta b}\Delta\delta_B \tag{28}$$

where the linearization constants $K_1 - K_9$, K_{pc}, K_{pe}, $K_{p\delta e}$, K_{pb}, $K_{p\delta b}$, K_{qc}, K_{qe}, $K_{q\delta e}$, K_{qb}, $K_{q\delta b}$, K_{vc}, K_{ve}, $K_{v\delta e}$, K_{vb}, $K_{v\delta b}$, K_{ce}, $K_{c\delta e}$, K_{cb} and $K_{c\delta b}$ are functions of the system parameters and the initial operating conditions. The state space model of power system is given by:

$$\Delta\dot{X} = A\Delta X + B\Delta U \tag{29}$$

where the state vector ΔX and control vector ΔU are:

$$\Delta X = \left[\Delta\delta \quad \Delta\omega \quad \Delta\dot{E}_q \quad \Delta E_{fd} \quad \Delta V_{dc}\right]^{\mathrm{T}}, \qquad \Delta U = [\Delta m_E \quad \Delta\delta_E \quad \Delta m_B \quad \Delta\delta_B]^{\mathrm{T}}$$

The structure of the matrices A and B are:

$$A = \begin{bmatrix} 0 & \omega_b & 0 & 0 & 0 \\ -\frac{K_1}{M} & -\frac{D}{M} & -\frac{K_2}{M} & 0 & -\frac{K_{pc}}{M} \\ -\frac{K_4}{T'_{do}} & 0 & -\frac{K_3}{T'_{do}} & \frac{1}{T'_{do}} & -\frac{K_{qc}}{T'_{do}} \\ -\frac{K_5 K_a}{T_a} & 0 & -\frac{K_6 K_a}{T_a} & -\frac{1}{T_a} & -\frac{K_{vc} K_a}{T_a} \\ K_7 & 0 & K_8 & 0 & K_9 \end{bmatrix}, \quad B = \begin{bmatrix} 0 & 0 & 0 & 0 \\ -\frac{K_{pe}}{M} & -\frac{K_{p\delta e}}{M} & -\frac{K_{pb}}{M} & -\frac{K_{p\delta b}}{M} \\ -\frac{K_{qe}}{T'_{do}} & -\frac{K_{q\delta e}}{T'_{do}} & -\frac{K_{qb}}{T'_{do}} & -\frac{K_{q\delta b}}{T'_{do}} \\ -\frac{K_{ve} K_a}{T_a} & -\frac{K_{v\delta e} K_a}{T_a} & -\frac{K_{vb} K_a}{T_a} & -\frac{K_{v\delta b} K_a}{T_a} \\ K_{ce} & K_{c\delta e} & K_{cb} & K_{c\delta b} \end{bmatrix}$$

D. Eigen Value of the System without Stabilizer

From equation $|\lambda I - A| = 0$, the eigenvalues of the system are computed and given as:

$$\lambda_1 = -19.752, \quad \lambda_{2,3} = 0.0484 + 3.4508\text{i}, \quad \lambda_{3,4} = -0.13878 \pm 0.30433\text{i}$$

The eigenvalues of the matrix A shows that the system is unstable. A supplementary stabilizer is certainly required for stability of the power system.

III. CONTROLLER STRUCTURE FOR DAMPING OF POWER OSCILLATION

In order to overcome the LFO problem, supplemental control action applied to generator excitation in form of PSS or UPFC device in form of power oscillation damping POD controller. In order to generate appropriate damping torque the parameters of the four main control loops of the UPFC (m_E,δ_E, m_B and δ_B) must be modulated. This is illustrated in Fig. 2.

The POD controller has a structure that is similar to that of the PSS controller. Fig. 3 presents a sample block diagram of a POD controller. It contains three main blocks, i.e., the gain block, the washout filter block, and a double stage lead-lag phase compensators. The washout filter block serves as a high-pass filter to eliminate the DC offset of the POD output and prevent steady-state changes in the terminal voltage of the generator. From this perspective, the washout time Tω should have a value in the range of 1 to 20 seconds defined to the electromechanical oscillation modes and two blocks (lead-lag) phase compensators [3].

In this study, the time constants, Tω, T_2, and T_4, were assigned specific values of 10s, 0.1s, and 0.1s, respectively, while the parameters of the controller, i.e., K_N, T_1, and T_3 had to be determined.

The speed deviation Δω used as an input signal to the POD, and U_N is the controller output.

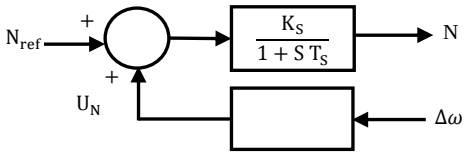

Fig. 2. UPFC with damping controller.

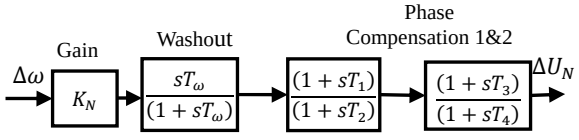

Fig. 3. Structure of power oscillation damping POD.

A. Design of Optimal controllers PSS and UPFC-POD

Improving dynamic stability of the power system against disturbances at different loading condition is the main objective of the coordinated design method. It can be achieved by suitable tuning of the parameters of multiple power system damping controllers between PSS and any one out from the four inputs controls channels of the series and shunt structure of UPFC device.

The problem of selecting damping controller's parameters independently and also through the simultaneous dual and triple-coordinated designs is solved by a CPSO optimization technique. This technique is dependent on eigenvalue–based objective function, which is formulated to recognize the minimum value of the damping ratio among all modes of the closed matrix. The POD controller is a lead-lag type. It can be described mathematically as:

$$U(s) = G(s)Y(s) \tag{30}$$

where G(s), Y(s) and U(s) are the POD controller transfer function, the POD input (measurement signal) and the POD output signal respectively. This output of the POD controller will provide additional damping by shifting modes to the left side. The Equation (30) can be expressed in state–space form as:

$$\Delta\dot{X}_C = A_C\Delta X_C + B_C\Delta U \tag{31}$$

where ΔX_C is the controller state vector. Equation (29) describes a linear model of the power system extracted around a certain operating point, combining equation (29) with equation (31), we obtained a closed-loop system.

$$\Delta\dot{X}_{C\ell} = A_{c\ell}\Delta X_{C\ell} \tag{32}$$

$$\Delta X_{C\ell} = \begin{bmatrix}\Delta X \\ \Delta X_C\end{bmatrix} \tag{33}$$

$$\zeta_i = -Real(\lambda_i)/|\lambda_i| \tag{34}$$

$$J = min(\zeta_i) \tag{35}$$

where $\Delta X_{C\ell}$ is the state vector of the closed loop system, λ_i is the ith eigenvalue (mode) of the closed loop matrix $A_{c\ell}$, ζ_i the damping coefficient of the ith eigenvalue. It is clear that the objective function J will identify the minimum value of the damping coefficient among modes.

The goal of optimization process is to maximize J in order to realize appropriate damping for all modes including electromechanical mode eigenvalue, by moving the dominant poles to the desired location, which enhance the system damping characteristics, and maximum J is searched within the limited range of control parameters.

$$K_L^{min} \le K_L \le K_L^{max}, \quad T_{Li}^{min} \le T_{Li} \le T_{Li}^{max}$$

where: $L = PSS, m_E, \delta_E, m_B, \delta_B$ and $i = 1, 3$
Typical ranges of K_L is 0.1– 100 and T_{Li} is 0.01–1.

IV. Optimization Algorithm

The problem of tuning the parameters for individual and coordinated design for multiple damping controllers, which would ensure the maximum damping performance was solved via a PSO optimization procedure. This promising technique appears as an effective solution of handling optimization problems. The PSO is a population-based, stochastic-optimization technique that was inspired by the natural characteristics of flocks of birds and schools of fish [31].

A. Classical PSO Technique

In PSO algorithm, every possible solution is represented as a particle. A group of particles comprises a population. Every particle keeps its position in hyperspace, which is related to the fittest solution.

These positions of the particles are saved in a special memory named pbest. Additionally, the change in the position of the particles is followed by the best value obtained at each iteration by any particle in the population is named gbest. For each iteration of the PSO algorithm, the pbest and gbest values are updated, and each particle changes its velocity toward them randomly. This concept can be described mathematically as follows:

$$v_{\mathrm{i}}^{k+1} = wv_{\mathrm{i}}^{k} + c_1 r_1\left(pbest_{\mathrm{i}} - x_{\mathrm{i}}^{k}\right) + c_2 r_2\left(gbest - x_{\mathrm{i}}^{k}\right) \tag{36}$$

$$x_{\mathrm{i}}^{k+1} = x_{\mathrm{i}}^{k} + v_{\mathrm{i}}^{k+1}\ ,\ \mathrm{i} = 1,2,\ldots,n, \tag{37}$$

where x and v are the position and the velocity of the particle respectively, w is the inertia weight factor, k is the number of iterations, c_1 and c_2 are the cognitive and asocial acceleration factors respectively, n is the number of particles, and r_1 and r_2 are the random numbers, which are uniformly-distributed within the range of 0 to 1 [32].

Fig. 4 shows the flowchart of the PSO algorithm for the tuning parameters of an individual and coordinated design.

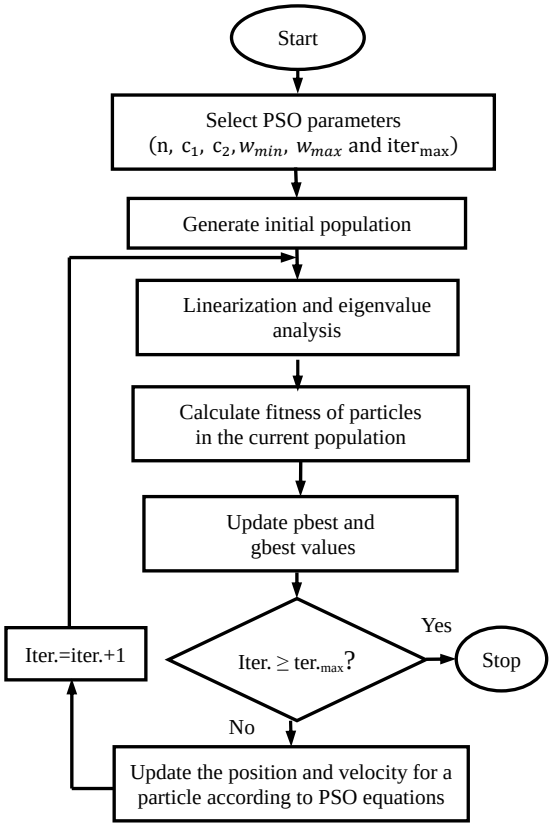

Fig. 4. PSO algorithm for the tuning parameters of an individual and coordinated design.

B. Chaotic Particle Swarm Optimization (CPSO)

Dependence of the simple PSO algorithm performance on its control parameters is one of the major disadvantages for achieving accurate optimization because it is not guaranteed to be global convergent. PSO and chaotic sequence techniques are combined to form a chaotic particle swarm optimization (CPSO) technique to increase the global searching ability of PSO algorithm. This combined method will help simple PSO to prevent premature convergence to local minima. The logistic equation, which is applied for hybrid PSO algorithm described as [33].

$$\beta^{k+1} = \mu\beta^{k}(1 - \beta^{k}), \qquad 0 \le \beta^{1} \le 1 \tag{38}$$

where μ is the control parameter in the range value between 0 to 4. Equation (38) is deterministic, it displays chaotic behavior when $\mu = 4$ and $\beta^{1} \notin \{0, 0.25, 0.5, 0.75, 1\}$. This prevents the dependence on initial conditions. The initial conditions are considered as the basic characteristic of chaos. The inertia weight factor in (36) is calculated by using the following equation:

$$w = w_{max} - [(w_{max} - w_{min})(iter/iter_{max})] \tag{39}$$

where w_{max} and w_{min} are maximum and minimum values of the inertia weight factor, $iter_{max}$ is the maximum number of iterations and $iter$ is the current iteration number. The new weight parameter w_{new} is defined by multiplying weight parameter w in (39) and logistic equation (38):

$$w_{new} = w \times \beta^{k+1} \tag{40}$$

To improve the global searching ability of PSO, we have introduced a new velocity update equation as follows:

$$v_{\mathrm{i}}^{k+1} = w_{new} v_{\mathrm{i}}^{k} + c_1 r_1 \left(pbest_{\mathrm{i}} - x_{\mathrm{i}}^{k}\right) + c_2 r_2 \left(gbest - x_{\mathrm{i}}^{k}\right) \tag{41}$$

We have observed and found that the weight in simple PSO algorithm decreases uniformly from w_{max} to w_{min}. However, the proposed new weight decreases and oscillates simultaneously for the total number of iterations. The final choice of a parameter was considered to be the optimal choice: swarm size, $iter_{max}$, c_1, c_2, w_{min}, w_{max}, μ and β^1 are chosen as 30, 100, 2, 2, 0.3, 0.9, 4 and 0.3 respectively.

V. Simulation And Comparison Results

In this section, the abilities of the proposed dual and triple coordinated designs are investigated in order to improve the dynamic stability of the power system through the damping of the LFO.

Figures 5-14 show the effect of applying the individual controllers and coordinated designs (dual/triple) for PSS and different UPFC-POD controllers in a SMIB of speed deviation with 10% step change in mechanical input power. The maximum overshoot as well as the settling time of the system responses should be studied to be compared to the capability of the simulated coordinate approaches in oscillation damping.

Figures 5, 6 demonstrate great improvement in damping system response while using the dual coordinated designs (PSS & m_E) and (PSS & m_B) over their individual control responses. Fig. 7 show an improvement in damping and deterioration in settling time of the system response while using the dual coordinated design (PSS & δ_B) over their individual control responses. Fig. 8 shows the best response in dual coordinated design while using the coordinated control (PSS & δ_E) over their individual control responses because it improved both damping parameters overshoot and settling time.

From figures 9, 10 and 11 it is clear that the triple coordinated design(PSS & m_B& δ_E), (PSS & m_E & δ_E) and (PSS & m_E & m_B) improves the system damping compared to the dual coordinated designs (PSS & m_B) and (PSS & δ_E); (PSS & m_E) and (PSS & δ_E); (PSS & m_E) and (PSS & m_B), respectively. Fig. 12 shows great improvement in settling time and deterioration of overshoot of the system response while using the triple coordinated design (PSS & δ_E & δ_B) over the dual coordinated design responses (PSS & δ_E) and (PSS & δ_B). Fig. 13 and Fig. 14 show improvement in overshoot and deterioration of settling time of the system response while using the triple coordinated designs (PSS & m_E & δ_B) and (PSS & m_B& δ_E) over the dual coordinated design responses (PSS & m_E) and (PSS & δ_B); (PSS & m_B) and (PSS & δ_E).

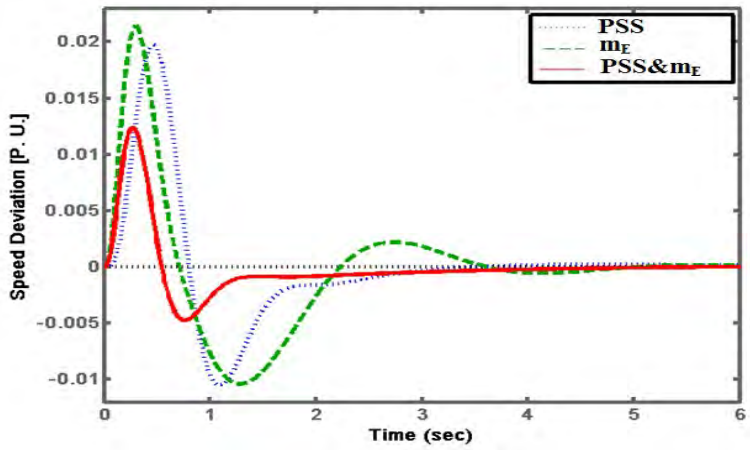

Fig. 5. Speed variation responses for multiple damping controllers individual and dual coordinated design (PSS, m_E, PSS & m_E).

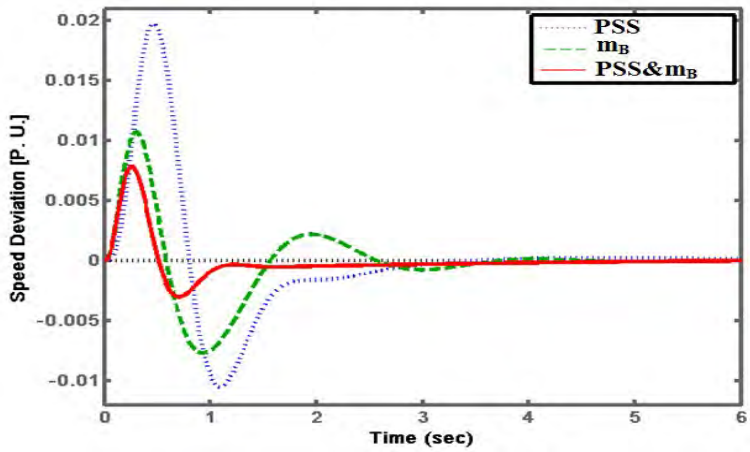

Fig. 6. Speed variation responses for multiple damping controllers individual and dual coordinated design (PSS, m_B, PSS & m_B).

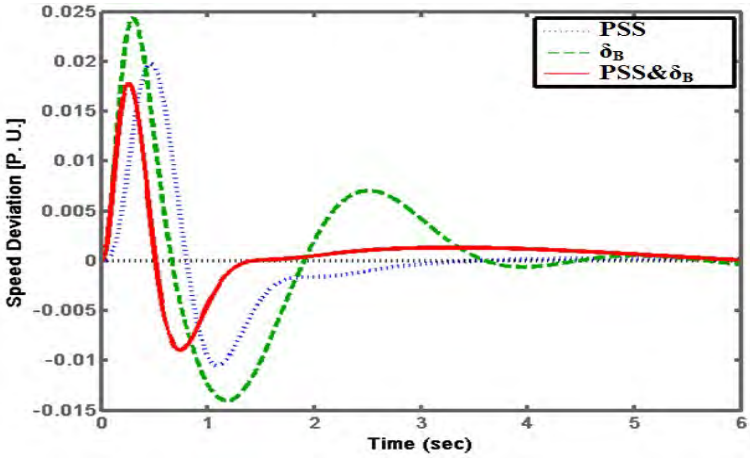

Fig. 7. Speed variation responses for multiple damping controllers individual and dual coordinated design (PSS, δ_B, PSS & δ_B).

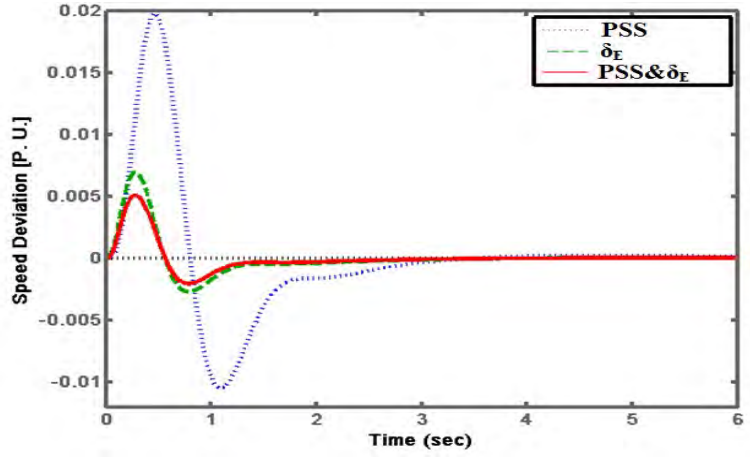

Fig. 8. Speed variation responses for multiple damping controllers individual and dual coordinated design (PSS, δ_E, PSS & δ_E).

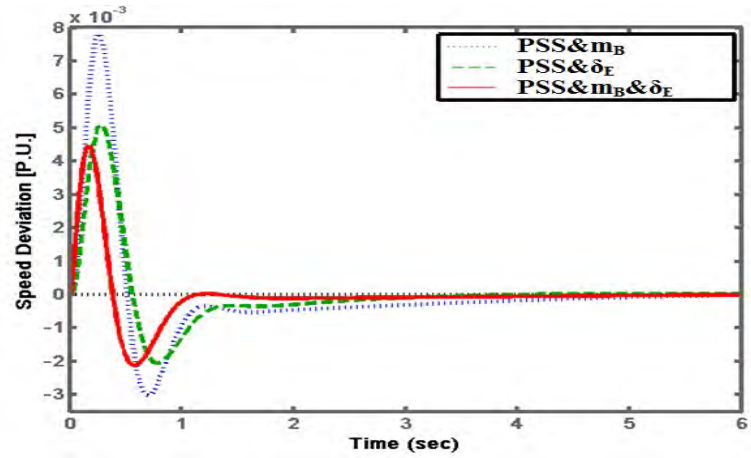

Fig. 9. Speed variation responses for dual and triple coordinated design with multiple damping controllers (PSS, m_B, δ_E).

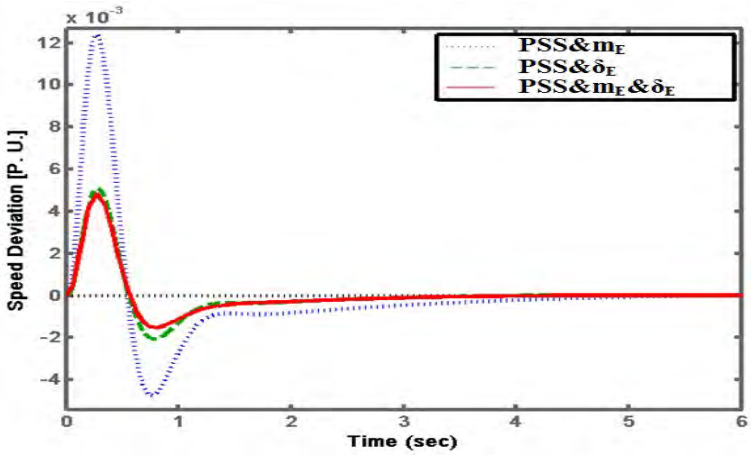

Fig. 10. Speed variation responses for dual and triple coordinated design with multiple damping controllers (PSS, m_E, δ_E).

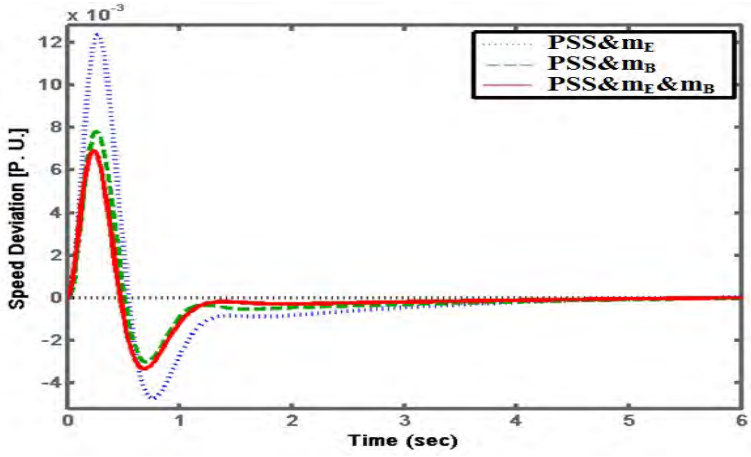

Fig. 11. Speed variation responses for dual and triple coordinated design with different damping controllers (PSS, m_E, m_B).

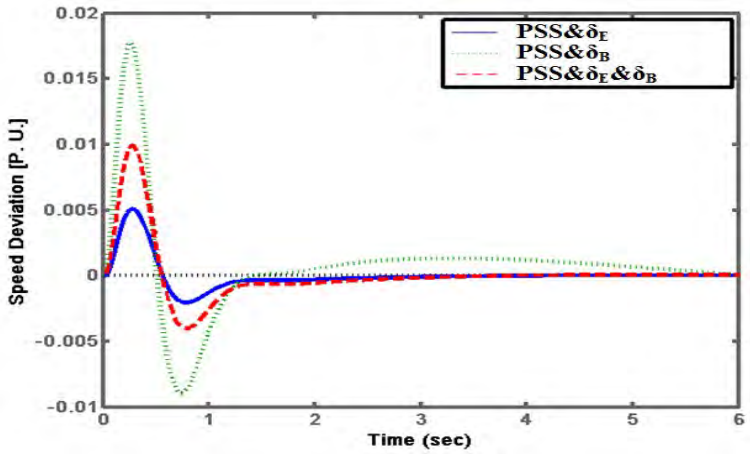

Fig. 12. Speed variation responses for dual and triple coordinated design with multiple damping controllers (PSS, δ_E, δ_B).

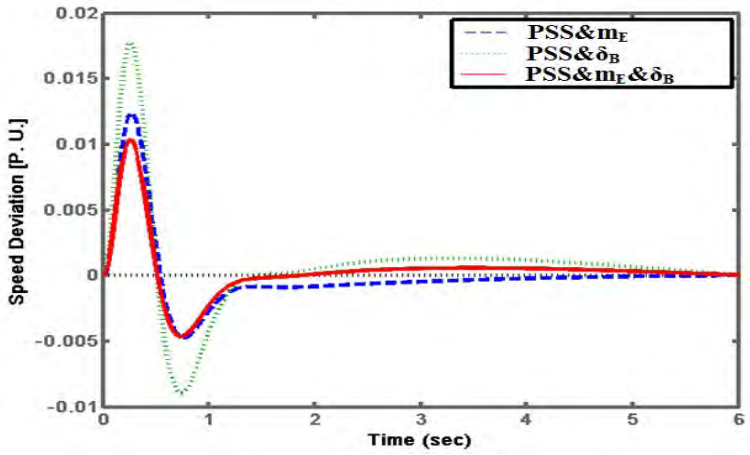

Fig. 13. Speed variation responses for dual and triple coordinated design with multiple damping controllers (PSS, m_E, δ_B).

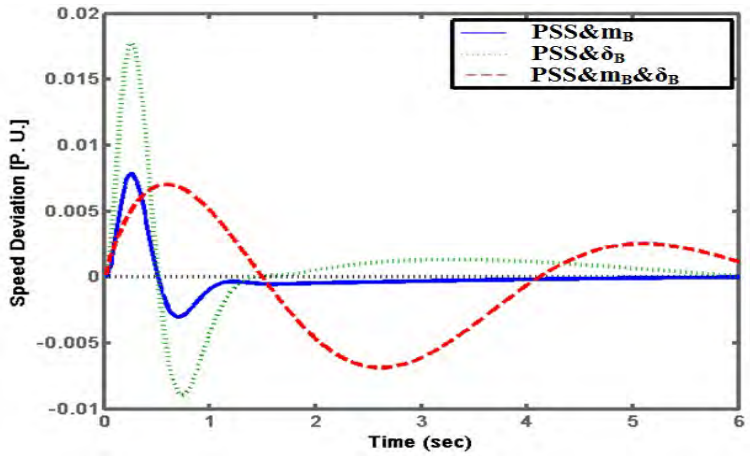

Fig. 14. Speed variation responses for dual and triple coordinated design with multiple damping controllers (PSS, m_B, δ_E).

VI. CONCLUSION

In this paper, we have focused on damping of LFO via PSS and UPFC-based POD applied independently and also through the simultaneous dual and triple-coordinated designs of the multiple damping controllers in a SMIB power system. To improve the ability of global searching and avoiding a slide into the premature convergence to local minima, CPSO is formed by combining the chaos theory and a simple PSO. For the proposed damping controller design problem, a CPSO algorithm was used as the optimization technique to search for the optimal damping controller parameters in both the individual and the coordinated designs. The simulation results showed the dual/triple coordinated designs (PSS & δ_E),(PSS & m_E), (PSS & m_B), (PSS & m_B & δ_E), (PSS & m_E & δ_E) and (PSS & m_E& m_B) provide robust damping effects over their individual control responses. The dual/triple coordinated designs (PSS & δ_B), (PSS & δ_E & δ_B), (PSS & m_E & δ_B) and (PSS & m_B & δ_B) demonstrate an unbalance improvement in the damping parameters in terms of overshoot and settling time system responses by improving one and deteriorate the other. Finally, the best triple-coordinated designs (PSS & m_B& δ_E), (PSS & m_E & δ_E) and (PSS & m_E & m_B) provide superior performance in comparison with the best dual-coordinated design (PSS & δ_E).

APPENDIX

Power system parameters (resistance, reactance, capacitance and voltage are in p.u. and time constants are in seconds):

Generator: $M = 8$, $T'_{do} = 5.044$, $X_q = 0.6$, $X_d = 1$, $\dot{X}_d = 0.3$, D=0.

Excitation: $K_a = 10$, $T_a = 0.05$.

Transmission line: $X_{tE} = 0.1$, $X_{BV} = 0.3$.

Operating condition: $P_e = 0.8$ p. u, $V_t = 1$, $V_b = 1$.

UPFC Transformers: $X_E = 0.1$, $X_B = 0.1$.

DC link parameter: $V_{dc} = 2$, $C_{dc} = 1$.

UPFC: $m_B = 0.0789$, $m_E = 0.4013$, $\delta_B = -78.217^0$, $\delta_E = -85.3478^0$, $K_S = 1$, $T_S = 0.05$.

REFERENCES

[1] H. Shayeghi, H. A. Shayanfar, S. Jalilzadeh, and A. Safari, "Design of output feedback UPFC controller for damping of electromechanical oscillations using PSO," *Energ. Convers. Manage.*, vol. 50, no. 10, pp. 2554–2561, Oct. 2009.

[2] C. Guo, and Q.-Z. Li, "Simultaneous coordinated tuning of PSS and FACTS damping controllers using improved particle swarm optimization," in *Proc. 2009 Asia-Pacific Power and Energy Engineering Conf.* (APPEEC 2009), Wuhan University, 2009. pp. 1-4.

[3] P. Kundur, *Power System Stability and Control*. India, McGraw-Hill Education, 1994, pp. 699-717.

[4] H. A. F. Almurib, L. H. Hassan, and M. Moghavvemi, "Design of robust power system stabilizers for Iraqi power network," in *Proc. SICE Annual Conf.*, Tokyo, 2011, pp. 1426-1429.

[5] P. Kumkratug, "Power system stability enhancement using unified power flow controller," *Amer. J. Appl. Scien.*,vol. 7, no. 11, pp. 1504 – 1508, Dec. 2010.

[6] A. Safari, "Multi-objective design of damping controllers with regional pole placement," *Int. J. Adv. Ren. Energy Res.*, vol. 1, no. 7, pp. 409-418, Aug. 2012.

[7] L. H. Hassan, M. Moghavvemi, H. A. F. Almurib, K. M. Muttaqi, and H. Duc, "Damping of low-frequency oscillations and improving power system stability via auto-tuned PI stabilizer using Takagi–Sugeno fuzzy logic," *Int. J. Elect. Power Energy Syst.*, vol. 38, no. 1, pp. 72-83, Jun. 2012.

[8] Y. L. Abdel-Magid, and M. A. Abido, "Robust coordinated design of excitation and TCSC-based stabilizers using genetic algorithms," *Electr. Pow. Syst. Res.*, vol. 69, no. 2-3, pp. 129–141, May 2004.

[9] S. A. Taher, R. Hemmati, A. Abdolalipour, and S. Akbari, "Comparison of different robust control methods in design of decentralized UPFC controllers," *Int. J. Elect. Power Energy Syst.*, vol. 43, no. 1, pp. 173-184, Dec. 2012.

[10] D. Rasolomampionona, and S. Anwar, "Interaction between phase shifting transformers installed in the tie-lines of interconnected power systems and automatic frequency controllers," *Int. J. Electr. Power Energy Syst.*, vol. 33, no. 8, pp. 1351-1360, Oct. 2011.

[11] M. Nayeripour, M. R. Narimani, T. Niknam, and S. Jam, "Design of sliding mode controller for UPFC to improve power oscillation damping," *Appl. Soft. Comput.*, vol. 11, no. 8, pp.4766-4772, Dec. 2011.

[12] M. R. Qader, "Evaluation of UPFC and ASVC applied to nonlinear load model," *Compel-Int. J. Comp. Math. Electr. Electron. Eng.*, vol. 25, no. 4, pp. 1019 – 1030, Dec. 2006.

[13] H. F. Wang, and H. Z. Xu, "FACTS-based stabilizers to damp power system oscillations - a survey," in *Proc. The 39th Int. Universities Power Engineering Conf.* (UPEC 2004), Bristol, UK, 2004.

[14] S. Panda, and N. P. Padhy, "Optimal location and controller design of STATCOM for power system stability improvement using PSO," *J. Frankl. Inst.-Eng. Appl. Math.*, vol. 345, no. 2, pp. 166-181, Mar. 2008.

[15] XP. Zhang, C. Rehtanz, and B. Pal, *Flexble AC Transmission system: Modeling and Control*. Springer, 2006, ch. 10.

[16] A. Aghazade, A. Kazemi, and M. M. Alamuti, "Coordination among FACTS POD and PSS controllers for damping of power system oscillations in large power systems using genetic algorithm," in *Proc. 2010 45th Int. Universities Power Engineering Conf.* (UPEC 201 0), 2010, pp. 1-6.

[17] R. Segal, A. Sharma, and M. L. Kothari, "A self-tuning power system stabilizer based on artificial neural network," *Int. J. Electr. Power Energy Syst.*, vol. 26, no. 3, pp. 423–430, Jul. 2004

[18] T. T. Nguyen, and R. Gianto, "Neural networks for adaptive control coordination of PSSs and FACTS devices in multimachine power system," *IET Gener. Transm. Distrib.*, vol. 2, no. 3, pp. 355–372, Mar. 2008.

[19] L. Rouco, "Coordinated design of multiple controllers for damping power system oscillations," *Int. J. Electr. Power Energy Syst.*, vol. 23, no. 7, pp. 517-530, Oct. 2001.

[20] V. Mukherjee V, and S. P. Ghoshal, "Comparison of intelligent fuzzy based AGC coordinated PID controlled and PSS controlled AVR system," *Int. J. Electr. Power Energy Syst.*, vol. 29, no. 9, pp. 679-689, Nov. 2007.
[21] A. Kazemi, and V. M. Sohrforouzani, "Power system damping using fuzzy controlled facts devices," *Int. J. Electr. Power Energy Syst.*, vol. 28, no. 5, pp. 349-357, Jun. 2006.
[22] S. M. Abd-Elazim, and E. S. Ali, "Coordinated design of PSSs and SVC via bacteria foraging optimization algorithm in a multimachine power system," *Int. J. Electr. Power Energy Syst.*, vol. 41, no. 1, pp. 44-53, Oct. 2012.
[23] S. Mohagheghi, G. K. Venayagamoorthy, and R. G. Harley, "Optimal neuro-fuzzy external controller for a STATCOM in the 12-bus benchmark power system," *IEEE Trans. Power Deliv.*, vol. 22, no. 4, pp. 2548-2558, Oct. 2007.
[24] H. E. A. Talaat, A. Abdennour, and A. A. Al-Sulaiman, " Design and experimental investigation of a decentralized GA-optimized neuro-fuzzy power systemstabilizer," *Int. J. Electr. Power Energy Syst.*, vol. 32, no. 7, pp. 751-759, Sep. 2010.
[25] H. E. Mostafa, M. A. El-Sharkawy, A. A. Emary, and K. Yassin, "Design and allocation of power system stabilizers using the particle swarm optimization technique for an interconnected power system," *Int. J. Electr. Power Energy Syst.*, vol. 34, no. 1, pp. 57-65, Jan. 2012.
[26] W. Du, X. Wu, H. F. Wang, and R. Dunn, "Feasibility study to damp power system multi-mode oscillations by using a single FACTS device," *Int. J. Electr. Power Energy Syst.*, vol. 32. no. 6, pp. 645-655, Sep. 2010.
[27] R. Hemmati, S. M. S. Boroujeni, E. Behzadipour, and H. Delafkar, "Supplementary stabilizer design based on STATCOM,'' *Indian J. Scien. Technol.*, vol. 4, no. 5, pp. 525-529, May 2011.
[28] A. T. Al-Awami, Y. L. Abdel-Magid, and M. A. Abido, "A particle-swarm-based approach of power system stability enhancement with unified power flow controller," *Int. J. Electr. Power Energy Syst.*, vol. 29, no.3, pp. 251-259, Mar. 2007.
[29] Y. Yao, *Electric Power System Dynamics*, NY: Academic Press, 1983, pp. 256.
[30] I. Kamwa, G. Trudel, and L. Gérin-Lajoie, "Robust design and coordination of multiple damping controllers using nonlinear constrained optimization," *IEEE Trans. Power Syst.*, vol. 15, pp. 1084–1092, Aug. 2000.
[31] J. Kennedy, and R. C. Eberhart,"Particle swarm optimization," in *Proc. of the IEEE Int.Conf. on Neural Networks*, 1995, pp. 1942–1948, 1995.
[32] E. Babaei, and V. Hosseinnezhad, "A QPSO based parameters tuning of the conventional power system stabilizer," in *Proc. of 2010 9th Int. Power and Energy Conf.* (IPEC 2010), Singapore, 2010, pp. 467 – 471.
[33] M. Eslami, H. Shareef, A. Mohamed, and M. Khajehzadeh, "Coordinated design of PSS and SVC damping controller using CPSO," in *Proc. 5th Int. Power Engineering and Optimization Conf.*, Selangor Malaysia, 2011, pp. 11-16.